interfacial dielectric constant will probably be between that of Si and SiO_2. The altered dielectric layers are not accounted for in our ellipsometric measurements, in which we assume that the oxide has only the dielectric constant of bulk SiO_2. This is probably why ellipsometry has underestimated the width of the oxides in Fig. 3.

The probe localization is obtained by constructing a wavepacket with a transverse momentum spread of more than a reciprocal lattice vector, and consequently all electronic momentum information is lost (as required by the uncertainty principle). Therefore these evanescent states responsible for tunnelling through the oxide and the states from the extended conduction band are treated on an equal footing, and cannot be separated in such a local measurement. In the simplest model, the silicon wavefunctions decay exponentially into the oxide barrier with a decay length for the evanescent states, $\lambda(E)$, determined by the energy difference between the interfacial state (E) and the conduction band edge of bulk SiO_2, (E_c), as $\lambda(E) = \hbar/\sqrt{(E_c - E)}$. The tunnelling current depends on the overlap of the evanescent states from either interface. A satisfactory tunnelling barrier is formed when the oxide thickness t is 6λ. This sets an absolute minimum thickness of $t_{min} = 0.7$ nm for an ideal SiO_2 gate oxide. Interfacial roughness adds another $6\sigma_r$ to t_{min}. The smallest roughness for our thermally grown oxides was $6\sigma_r = 0.6$ nm which puts a lower limit of 1.2 nm on the practical SiO_2 gate oxide thickness. The induced gap states also place severe constraints on the minimum allowed thickness for alternative dielectrics, many of which have large dielectric constants, but reduced bandgaps and hence longer decay lengths. Furthermore, there is the possibility of a reaction between the dielectric and the silicon substrate to form a silicon oxide interlayer. If the interlayer thickness exceeds 1.3 nm (and a typical native oxide is 2 nm thick), the gate capacitance is less than what could be obtained with a pure SiO_2 gate oxide. □

Received 20 January; accepted 8 April 1999.

1. Semiconductor Industry Association *The National Technology Roadmap for Semiconductors* 71–81 (Sematech, Austin, 1997).
2. Timp, G. *et al.* in *IEDM Technical Digest* 615–618 (IEDM, San Francisco, 1998).
3. Cryot-Lackmann, F. Sur le calcul de la cohesion et de la tension superficielle des mataux de transition par une methode de liasions fortes. *J. Phys. Chem. Solids* **29,** 1235–1243 (1968).
4. Ourmazd, A., Taylor, D. W., Rentschler, J. A. & Bevk, J. Si to SiO_2 transformation: interfacial structure and mechanism. *Phys. Rev. Lett.* **59,** 213–216 (1987).
5. Himpsel, F., McFeely, F. R., Taleb-Ibrahimi, A., Yarmoff, J. A. & Hollinger, G. Microscopic structure of the SiO_2/Si interface. *Phys. Rev. B* **38,** 6084–6096 (1988).
6. Grunthaner, F. J. & Grunthaner, P. J. Chemical and electronic structure of the Si/SiO_2 interface. *Mater. Sci. Rep.* **1,** 65–160 (1986).
7. Pasquarello, A., Hybertsen, M. S. & Car, R. Theory of Si 2p core-level shifts at the Si(001)-SiO_2 interface. *Phys. Rev. B* **53,** 10942–10950 (1996).
8. McFeely, F. R., Zhang, K. Z., Banaszak Holl, M. M., Lee, S. & Bender, J. E. An inquiry concerning the principles of the Si 2p core-level photoemission shift assignments at the Si/SiO_2 interface. *J. Vac. Sci. Technol. B* **14,** 2824–2830 (1996).
9. Muller, D. A., Tzou, Y., Raj, R. & Silcox, J. Mapping sp^2 and sp^3 states of carbon at sub-nanometre spatial resolution. *Nature* **366,** 725–727 (1993).
10. Muller, D. A., Subramanian, S., Sass, S. L., Silcox, J. & Batson, P. E. Near atomic scale studies of electronic structure at grain boundaries in Ni_3Al. *Phys. Rev. Lett.* **75,** 4744–4747 (1995).
11. Batson, P. E. Simultaneous STEM imaging and electron energy-loss spectroscopy with atomic column sensitivity. *Nature* **366,** 727–728 (1993).
12. Browning, N. D., Chisholm, M. M. & Pennycook, S. J. Atomic-resolution chemical analysis using a scanning transmission electron microscope. *Nature* **366,** 143–146 (1993).
13. Muller, D. A. & Silcox, J. Delocalization in inelastic scattering. *Ultramicroscopy* **59,** 195–213 (1995).
14. Egerton, R. F. *Electron Energy Loss Spectroscopy in the Electron Microscope* 2nd edn (Plenum, New York, 1996).
15. Colliex, C. & Jouffrey, B. Diffusion inelastique des electrons dans une solide par excitation de niveaus atomiques profonds. *Phil. Mag.* **25,** 491–514 (1972).
16. Müller, J. E. & Wilkins, J. Band-structure approach to the x-ray spectra of metals. *Phys. Rev. B* **29,** 4331–4348 (1984).
17. Muller, D. A. *et al.* Atomic scale observations of metal-induced gap states at {222} MgO/Cu interfaces. *Phys. Rev. Lett.* **80,** 4741–4744 (1998).
18. Brown, G. E. Jr, Waychunas, G. A., Stohr, J. & Sette, F. Near-edge structure of oxygen in inorganic oxides: effect of local geometry and cation type. *J. Phys.* **47,** (Colloque C8) 685–689 (1986).
19. Wallis, D., Gaskell, P. H. & Brydson, R. Oxygen K near-edge spectra of amorphous silicon suboxides. *J. Microsc.* **180,** 307–312 (1993).
20. Zangwill, A. *Physics at Surfaces* (Cambridge Univ. Press, New York, 1988).

Acknowledgements. We thank D. R. Hammann, M. S. Hybertsen, P. Rez, J. Neaton and B. Batlogg for discussions, and J. Silcox and M. Thomas for access to the Cornell Center for Materials Research STEM. Funding for the operation and acquisition of the STEM was provided by the NSF. Upgrades were founded by the US Air Force Office of Scientific Research. The X-ray diffraction was performed on X16B at the National Synchrotron Light Source.

Correspondence and requests for materials should be addressed to D.A.M. (e-mail: davidm@bell-labs.com).

Molecular mechanistic origin of the toughness of natural adhesives, fibres and composites

Bettye L. Smith*†, Tilman E. Schäffer‡†, Mario Viani*, James B. Thompson*, Neil A. Frederick*, Johannes Kindt*, Angela Belcher§, Galen D. Stucky‖, Daniel E. Morse¶ & Paul K. Hansma*

** Department of Physics, ‖ Department of Chemistry and Materials, and ¶ Department of Molecular, Cellular, and Developmental Biology, University of California at Santa Barbara, California 93106, USA*
‡ Department of Molecular Biology, Max-Planck-Institute for Biophysical Chemistry, 37070 Göttingen, Germany
§ Department of Chemistry, The University of Texas at Austin, Austin, Texas 78712, USA
† These authors contributed equally to this work

Natural materials are renowned for their strength and toughness[1–5]. Spider dragline silk has a breakage energy per unit weight two orders of magnitude greater than high tensile steel[1,6], and is representative of many other strong natural fibres[3,7,8]. The abalone shell, a composite of calcium carbonate plates sandwiched between organic material, is 3,000 times more fracture resistant than a single crystal of the pure mineral[4,5]. The organic component, comprising just a few per cent of the composite by weight[9], is thought to hold the key to nacre's fracture toughness[10,11]. Ceramics laminated with organic material are more fracture resistant than non-laminated ceramics[11,12], but synthetic materials made of interlocking ceramic tablets bound by a few weight per cent of ordinary adhesives do not have a toughness comparable to nacre[13]. We believe that the key to nacre's fracture resistance resides in the polymer adhesive, and here we reveal the properties of this adhesive by using the atomic force microscope[14] to stretch the organic molecules exposed on the surface of freshly cleaved nacre. The adhesive fibres elongate in a stepwise manner as folded domains or loops are pulled open. The elongation events occur for forces of a few hundred piconewtons, which are smaller than the forces of over a nanonewton required to break the polymer backbone in the threads. We suggest that this 'modular' elongation mechanism might prove to be quite general for conveying toughness to natural fibres and adhesives, and we predict that it might be found also in dragline silk.

We have looked for the mechanism behind the toughness of the organic adhesives and fibres, and, in particular, at the nacre in abalone shells. Analysis of the insoluble organic matrix from the abalone shell revealed a fibrous core in the interlamellar sheets placed between successive nacre tablets[5,15,16], which probably serve as an adhesive holding the tablets together. The organic adhesive is readily apparent when the tablets are pulled apart (Fig. 1). At least one protein, lustrin A, has been isolated from this insoluble organic matrix. The complementary DNA and translated protein sequence reveal that the structure of this protein consists of about 10 alternating and highly conserved cysteine-rich and proline-rich domains, demonstrating that the structure is highly modular[17]. Immunohistochemical analysis of the fibres (Fig. 1) revealed lustrin A to be a component of the adhesive between the nacre mineral tablets.

Rief *et al.*[18,19] demonstrated that the modular structure of a single molecule can be examined by attaching the molecule between a flat surface and a cantilever of an atomic force microscope (AFM). By pulling on the protein titin and plotting the force versus extension curves, these authors measured the force required to break open the individual subunit in its modular structure. As the titin

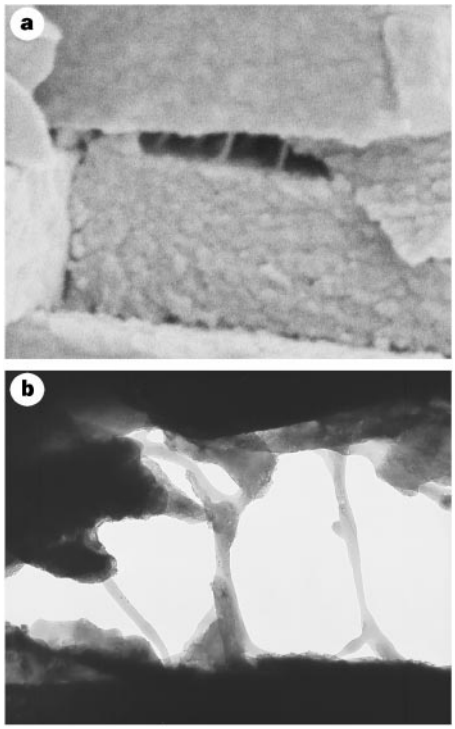

Figure 1 Scanning and transmission electron micrographs of a freshly cleaved abalone shell, showing adhesive ligaments formed between nacre tablets. **a**, Scanning electron micrograph of a freshly cleaved abalone shell showing adhesive ligaments formed between consecutive abalone nacre tablets on exertion of mechanical stress. The tablets are ~400 nm thick. **b**, Transmission electron micrograph of another cleaved abalone shell, showing the adhesive ligaments between nacre tablets. The space between the tablets is ~600 nm. Thus the ligaments can lengthen to many times the original spacing between the tablets, which is of the order of 30 nm.

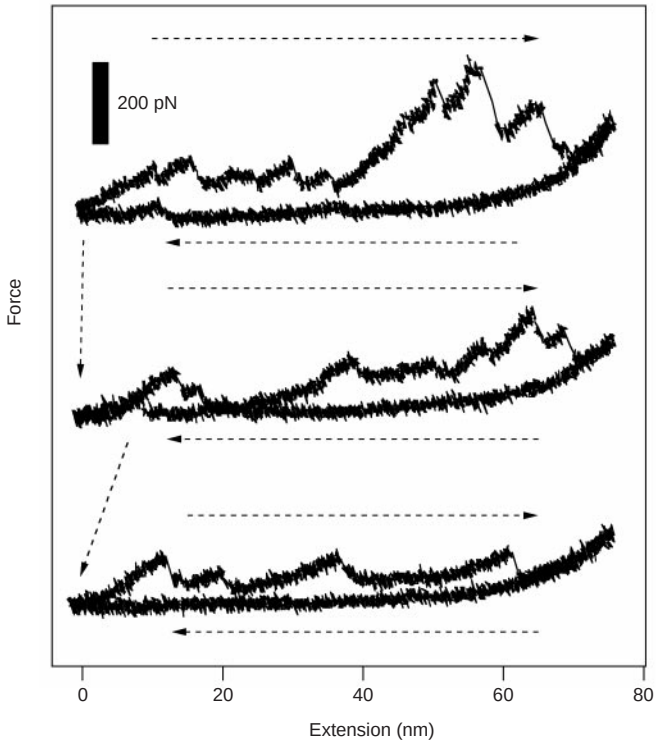

Figure 2 Consecutive force–extension curves, obtained using an atomic force microscope, from pulling on a freshly cleaved abalone nacre surface. Rupture events, with a sawtooth appearance, are visible in each of the curves. The surface was not touched between pulls, strong evidence that some refolding took place, possibly of domains in lustrin A. The approach and retract curves show hysteresis, indicating that the rupture events dissipate energy.

molecule was stretched, the force–extension curve revealed a sawtooth pattern. Using titin constructs, Rief *et al.*[19] demonstrated that every peak in the sawtooth pattern corresponded to a single domain unfolding. Apparently, it is the cumulative effect of the intermediate-strength hydrophobic bonds in the immunoglobulin-like domains of titin which contribute to the sawtooth force–distance curves found for this molecule[20,21]. Studies using optical tweezers corroborated these results[22–24]. These initial studies demonstrate that individual titin subunits unfold one at a time, suggesting that this technique affords an opportunity to delineate some of nature's mechanisms in building modular elastic fibres.

We have used this technique to investigate the molecules that hold abalone shells together. Figure 2 shows force–extension curves for the organic material exposed on a freshly cleaved nacre surface. Breaking forces of the order of 100–400 pN are seen in these curves. The hysteresis observed after a complete pulling cycle demonstrates that work has been done on the shell. This work is irreversibly dissipated as heat, and the area between the retracting and the approaching parts of the curve quantifies this heat. In this case, the dissipated heat is of the order of $(0.4–1) \times 10^{-17}$ J per cycle (Fig. 2). The sawtooth-like force–extension curves, and the observation that we could repeatedly unfold molecule(s) without touching the surface between pulls, suggest that bonds of some kind are breaking and reforming. As lustrin A is present on that surface, it is possible that we observed unfolding of this protein. However, and this is the key point, the mechanism behind the strength and toughness of the adhesive is revealed by the force–extension curves and does not depend on the identification of the specific molecules involved. This behaviour may reflect the successive opening of intra-chain loops or folded domains within a single molecule, or the successive release of sacrificial inter-chain bonds holding a crosslinked multichain matrix together.

To demonstrate the effect that a material with this type of force–extension curve can have on the properties of an adhesive made from modular fibres, we consider three different cases. Gluing materials together with conventional adhesives has traditionally involved either relatively stiff adhesives such as epoxies, or elastic adhesives such as silicon adhesives. When pulling on two surfaces glued together with a short molecule, the pulling force increases rapidly with only a little extension of the molecule (Fig. 3). First, a perfect stiff adhesive would be a short molecule bound to each surface by strong (that is, covalent or ionic) bonds and the molecules of the adhesive itself would be held together with strong bonds. Thus the break strength of each adhesive molecule would be the force required to break a strong bond: of the order of one nanonewton (estimated by dividing one electron volt by an extension of one ångström). For a material with many strongly bound molecules in parallel, the macroscopic tensile strength is expected to be of the order of several gigapascals. This is the order of magnitude for the breaking force of strong polymers such as Kevlar[25,26]. The fracture toughness of such materials is rather small, however, even though the forces are large. This can be understood by considering the area under the force–extension curve (Fig. 3), which is the energy required to break the material. Because those stiff materials have a small elastic strain, the extension over which the force must be exerted until it breaks is small. Therefore the area under the curve, or the energy required to break the material, is small (Fig. 3).

Second, in contrast to this behaviour, the idealized curve for an elastic fibre made of long molecules shows that the force increases

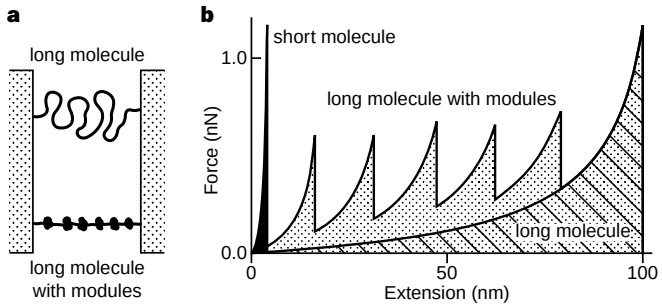

Figure 3 Model of long polymers and force–extension curves for different kinds of polymers. **a**, Diagram of long polymers behaving as entropic springs. The lower molecule is compacted, with many domains that are held together with intermediate-strength sacrificial bonds. **b**, Force–extension curves for three different kinds of molecules. A short molecule (solid curve) resists pulling up to a high force before it breaks at small extensions. The energy required to break this short molecule (area under the curve) is small. A long molecule (hatched curve) behaves like an entropic spring and yields to the pulling force up to large extensions. The energy to break the long molecule is larger than that for the small molecule, but the forces at low extensions are small. But a long molecule that is compacted into domains (the stippled plus the hatched curve) that are held together with intermediate-strength bonds resists pulling already at small extensions. Before the molecule's backbone can break at forces of the order of 1 nN, modules unfold at intermediate forces (0.1–0.7 nN). Repeated unfolding of molecules allows stretching up to large extensions, required significant energy. Therefore, a long molecule that is compacted into domains that are held together with intermediate-strength bonds combines both high (tensile) strength and high toughness.

slowly as the elastic material is stretched to the point at which the elastic limit is reached (Fig. 3)[27,28]. Then the force increases rapidly for further extension until it breaks. This break will again occur at a force of the order of one nanonewton per molecular chain, assuming each chain is bound to each surface with a strong bond and is itself held together by strong bonds. Contrary to the case of short, inelastic molecules, the pulling force must be applied over much larger extensions. Therefore, the area under the force–extension curve would be larger (Fig. 3), and thus more energy would be needed to break the material. Unfortunately, the technology does not at present exist for making such an idealized elastic material. Real elastic materials such as rubbers have tensile strengths that correspond to breaking forces per molecule of the order of 0.1% of the theoretical maximum. But even if ideal elastic materials could be produced, there would still be a significant advantage to incorporating nature's mechanism of tying up most of the molecule's length with intermediate-strength sacrificial bonds.

Third, an adhesive or fibre that combines the best of both worlds would display a force–extension curve that rises to a large force quickly, but then maintains that force over large extensions. It would consist of long molecules with many domains that are either folded or looped, with intermediate-strength bonds (of the order of 0.1–0.7 nN) compacting the molecule. These intermediate-strength bonds are stronger than individual hydrogen bonds or van der Waals bonds, but weaker than covalent bonds. Alternatively, these may represent the cumulative effect of multiple weak bonds (either intra- or interchain) acting in concert. For such a molecule, the force rises quickly with extension (Fig. 3). But then, when the force rises to a significant fraction of the force required to break a strong bond and threatens to break the backbone of the molecule, a domain unfolds or a loop is opened, therefore avoiding the breaking of a strong bond in the backbone.

On further pulling, the force then again rises to a significant fraction of the force required to break a strong bond, but again, before a strong bond is broken, another domain unfolds. The process continues until all domains are unfolded (or loops are opened) and finally a strong bond breaks. The net result is to sustain a large force over the pulling extension, making it 'strong', while producing a relatively large area under the force–extension curve, making it 'tough' as well.

An approximate analogy to this process is found in Greek mythology: Sisyphus was condemned by Zeus to push a heavy rock up a mountain only to have it slip out of his hands and roll back to the bottom just before he reached the summit. In such a fall, the rock would dissipate its potential energy into heat, and Sisyphus had to start all over again. The case of extending a modular fibre is analogous. One needs to pull hard, and do work, but before the breaking point (the 'summit') is reached, a domain unfolds or a loop opens, and the energy stored in the fibre is dissipated as heat. Then, the fibre has to be pulled on again, until the next domain breaks and so on, until no folded domains are left and the fibre at least breaks. (We note that if the force is relaxed before the fibre breaks, the domains or loops can reform as shown in Fig. 2.) In natural materials, proteins provide the modular fibre: but this mechanism should work for other polymers, as long as it is possible to compact the length of the polymers using intermediate-strength bonds that break sacrificially with forces comparable to, but less than, the force of a nanonewton or so that breaks strong bonds in the polymer backbone. □

Received 26 February; accepted 20 April 1999.

1. Hinman, M., Dong, Z., Xu, M. & Lewis, R. V. in *Biomolecular Materials* (eds Viney, C., Case, S. T. & Waite, J. H.) 25–34 (Materials Research Soc., Pittsburgh, 1993).
2. Qin, X., Coyne, K. J. & Waite, J. H. A novel natural copolymer: A collagenous molecule from mussel byssus contains silk fibroin-like domains. *Am. Zool.* **37,** 125A (1997).
3. Waite, J. H., Qin, X. X. & Coyne, K. J. The peculiar collagens of mussel byssus. *Matrix Biol.* **17,** 93–106 (1998).
4. Currey, J. D. Mechanical properties of mother of pearl in tension. *Proc. R. Soc. Lond. B* **196,** 443–463 (1977).
5. Jackson, A. P., Vincent, J. F. & Turner, R. M. The mechanical design of nacre. *Proc. R. Soc. Lond. B* **234,** 415–440 (1988).
6. Heslot, H. Artificial fibrous proteins: A review. *Biochimie (Paris)* **80,** 19–31 (1998).
7. Vollrath, F. & Edmonds, D. T. Modulation of the mechanical properties of spider silk by coating with water. *Nature* **340,** 305–307 (1989).
8. Qin, X. X., Coyne, K. J. & Waite, J. H. Tough tendons. Musse byssus has collagen with silk-like domains. *J. Biol. Chem.* **272,** 32623–32627 (1997).
9. Watable, N. & Wilbur, K. M. (eds.) *The Mechanisms of Biomineralization in Invertebrates and Plants* (Univ. South Carolina Press, Columbia, SC, 1976).
10. Weiner, S. Organization of extracellularly mineralized tissues: a comparative study of biological crystal growth. *CRC Crit. Rev. Biochem.* **20,** 365–408 (1986).
11. Jackson, A. P., Vincent, J. F. V. & Turner, R. M. A physical model of nacre. *Composites Sci. Technol.* **36,** 255–266 (1989).
12. Clegg, W. J., Kendall, K., Alford, N. M., Button, T. W. & Birchall, J. D. A simple way to make tough ceramics. *Nature* **347,** 455–457 (1990).
13. Almqvist, N. *et al.* Methods for fabricating and characterizing a new generation of biomimetic materials. *Mater. Sci. Eng. C* **7(1),** 37–43 (1999).
14. Binnig, G., Quate, C. F. & Gerber, C. The atomic force microscope. *Phys. Rev. Lett.* **56,** 930–933 (1986).
15. Addadi, L. & Weiner, S. Biomineralization—A pavement of pearl. *Nature* **389,** 912–915 (1997).
16. Schäffer, T. E. *et al.* Does abalone nacre form by heteroepitaxial nucleation or by growth through mineral bridges? *Chem. Mater.* **9,** 1731–1740 (1997).
17. Shen, X., Belcher, A. M., Hansma, P. K., Stucky, G. D. & Morse, D. E. Molecular cloning and characterization of lustrin A, a matrix protein from shell and pearl nacre of *Haliotis rufescens*. *J. Biol. Chem.* **272,** 32472–32481 (1997).
18. Rief, M., Gautel, M., Oesterhelt, F., Fernandez, J. M. & Gaub, H. Single molecule force spectroscopy on polysaccharides by atomic force microscopy. *Science* **276,** 1295–1297 (1997).
19. Rief, M., Gautel, M., Oesterhelt, F., Fernandez, J. M. & Gaub, H. E. Reversible unfolding of individual titin immunoglobulin domains by AFM. *Science* **276,** 1109–1112 (1997).
20. Grandbois, M., Beyer, M., Rief, M., Clausen-Schaumann, H. & Gaub, H. E. How strong is a covalent bond? *Science* **283,** 1727–1730 (1999).
21. Mehta, A. D., Rief, M., Spudich, J. A., Smith, D. A. & Simmons, R. M. Single-molecule biomechanics with optical methods. *Science* **283,** 1689–1695 (1999).
22. Kellermayer, M. S., Smith, S. B., Granzier, H. L. & Bustamante, C. Folding-unfolding transitions in single titin molecules characterized with laser tweezers. *Science* **276,** 1112–1116 (1997).
23. Keller, T. C. S. Molecular bungees. *Nature* **387,** 233–235 (1997).
24. Tskhovrebova, L., Trinick, J., Sleep, J. A. & Simmons, R. M. Elasticity and unfolding of single molecules of the giant muscle protein titin. *Nature* **387,** 308–312 (1997).
25. Al-Hassani, S. T. S. & Kaddour, A. S. Strain rate effects on GRP, KRP and CFRP composite laminates. *Key Eng. Mater.* **141,** 427–452 (1998).
26. Greenwood, J. H. & Rose, P. G. Compressive behaviour of Kevlar 49 fibres and composites. *J. Mater. Sci.* **9,** 1809–1814 (1974).
27. Lu, H., Isralewitz, B., Krammer, A., Vogel, V. & Schulten, K. Unfolding of titin immunoglobulin domains by steered molecular dynamics simulation. *Biophys. J.* **75,** 662–671 (1988).
28. Slater, G. W., Hubert, S. J. & Nixon, G. I. Construction of approximate entropic forces for finitely extensible nonlinear elastic (FENE) polymers. *Macromol. Theory Simulat.* **3,** 695–704 (1994).

Acknowledgements. We thank F. Lange and E. Kramer for help in understanding polymers, and H. Gaub and his group members both for helping to teach us how to unfold proteins, and for suggesting that organic components of abalone shells might be a good system in which to study polymer unfolding. This work was supported by the NSF (P.K.H.), by NSF through the Materials Research Laboratory, the Office of Naval Research, the Army Research Office MURI program, and the NOAA National Sea Grant College Program.

Correspondence and requests for materials should be addressed to B.L.S. (e-mail: bettye@physics.ucsb.edu).